

Cite this: DOI: 00.0000/xxxxxxxxx

Supporting Information: Do Molecular Dynamics Force Fields Accurately Model Ramachandran Distributions of Amino Acid Residues in Water?[†]

Brian Andrews,^a Jose Guerra,^c Reinhard Schweitzer-Stenner^b, and
Brigita Urbanc^{*a}

Supporting Tables

Table S1: Experimental and calculated J coupling constants and the uncertainty values used in χ_J^2 calculations for all guest amino acid residues in GxG considered in this work. The MD-derived values for each of the three force fields are based on conformations within 50–300 ns of each trajectory.

	$^3J(H^N, H^{C_\alpha})$	$^3J(H^N, C')$	$^3J(H^{C_\alpha}, C')$	$^3J(C, C')$	$^1J(N, C_\alpha)$
GGG^a					
Experimental	5.89	1.10	4.01	0.26	12.17
Gaussian	5.94	1.16	3.95	0.66	11.78
Amber ff19SB	6.05	1.10	3.84	0.82	11.42
Amber ff14SB	5.97	1.14	3.55	0.99	11.40
OPLS-AA/M	6.01	1.05	3.25	1.25	11.60
CHARMM36m	5.99	1.17	3.93	0.60	11.69
Uncertainty	0.02	0.07	0.1	0.03	0.07
	$^3J(H^N, H^{C_\alpha})$	$^3J(H^N, C')$	$^3J(H^{C_\alpha}, C')$	$^3J(H^N, C_\beta)$	$^1J(N, C_\alpha)$
GAG^b					
Experimental	6.11	1.18	1.90	2.09	11.28
Gaussian	6.00	1.09	1.89	1.95	11.39
Amber ff19SB	5.91	1.51	1.76	1.69	10.96
Amber ff14SB	6.25	1.10	1.69	1.80	11.17
OPLS-AA/M	7.19	0.81	1.94	1.61	11.28
CHARMM36m	6.37	1.24	2.05	1.67	11.21
Uncertainty	0.02	0.07	0.1	0.03	0.07
GLG					
Experimental	6.78	0.84	2.45	1.75	10.96
Gaussian	6.72	1.01	2.36	1.69	11.11
Amber ff19SB	6.35	1.25	1.75	1.67	10.78
Amber ff14SB	6.58	0.95	2.20	1.79	10.95
OPLS-AA/M	7.39	0.62	2.09	1.66	11.04
CHARMM36m	6.61	0.97	2.03	1.75	11.02
Uncertainty	0.01	0.09	0.03	0.15	0.10
GVG					
Experimental	7.46	0.91	2.33	1.59	11.24
Gaussian	7.43	0.85	2.42	1.50	11.50
Amber ff19SB	6.75	1.45	2.12	1.36	10.72
Amber ff14SB	6.63	1.03	1.82	1.69	10.97
OPLS-AA/M	7.59	0.51	2.06	1.64	10.97
CHARMM36m	6.58	0.95	1.84	1.77	10.98
Uncertainty	0.02	0.07	0.1	0.06	0.07
GIG					
Experimental	7.47	0.86	2.34	1.40	10.88
Gaussian	7.33	0.90	2.41	1.50	10.97
Amber ff19SB	6.75	1.08	1.85	1.61	10.63
Amber ff14SB	6.43	0.92	1.75	1.85	10.96
OPLS-AA/M	7.47	0.64	2.03	1.61	11.10
CHARMM36m	6.71	0.93	1.92	1.73	10.86
Uncertainty	0.02	0.07	0.1	0.06	0.07
GFG					
Experimental	7.45	0.74	2.20	1.79	11.48
Gaussian	7.41	0.76	2.30	1.55	11.48
Amber ff19SB	6.24	1.66	1.71	1.43	11.08
Amber ff14SB	6.54	1.07	1.91	1.71	11.08

OPLS-AA/M	7.51	0.76	2.16	1.51	11.05
CHARMM36m	6.63	1.10	2.17	1.66	11.05
Uncertainty	0.02	0.24	0.27	0.17	0.10
GYG					
Experimental	7.37	0.74	2.47	1.37	11.26
Gaussian	7.49	0.78	2.58	1.51	11.38
Amber ff19SB	6.21	1.49	1.71	1.56	10.86
Amber ff14SB	6.43	1.22	2.10	1.66	11.40
OPLS-AA/M	7.48	0.82	2.25	1.48	11.05
CHARMM36m	6.55	1.18	1.91	1.63	10.96
Uncertainty	0.03	0.24	0.09	0.11	0.13
GD^PG					
Experimental	7.44	1.19	3.24	1.25	11.89
Gaussian	7.70	1.19	3.29	1.16	11.70
Amber ff19SB	7.65	1.43	3.64	1.03	10.23
Amber ff14SB	6.74	1.21	2.64	1.55	10.82
OPLS-AA/M	7.40	0.69	2.25	1.61	10.98
CHARMM36m	7.55	0.91	2.37	1.39	11.07
Uncertainty	0.02	0.09	0.24	0.28	0.05
GE^PG					
Experimental	6.99	0.94	2.07	1.59	11.24
Gaussian	7.02	0.88	2.16	1.64	11.07
Amber ff19SB	6.25	1.54	1.72	1.51	10.99
Amber ff14SB	6.70	1.18	2.20	1.58	10.99
OPLS-AA/M	7.42	0.75	2.09	1.56	11.10
CHARMM36m	6.81	1.28	1.88	1.45	11.02
Uncertainty	0.07	0.18	0.32	0.12	0.05
GRG					
Experimental	6.66	1.00	2.47	1.79	11.02
Gaussian	6.60	0.99	2.40	1.77	11.16
Amber ff19SB	6.10	1.41	1.68	1.66	10.72
Amber ff14SB	6.52	1.09	1.81	1.71	11.01
OPLS-AA/M	7.47	0.79	2.14	1.51	11.07
CHARMM36m	6.74	1.11	2.16	1.61	11.14
Uncertainty	0.01	0.08	0.05	0.15	0.10
GCG					
Experimental	7.29	0.87	2.79	1.89	11.81
Gaussian	7.09	0.89	2.81	1.63	11.56
Amber ff19SB	6.30	2.23	1.72	1.00	11.73
Amber ff14SB	6.30	1.09	1.94	1.81	10.98
OPLS-AA/M	7.23	0.79	2.22	1.61	11.00
CHARMM36m	6.46	1.11	2.08	1.73	11.04
Uncertainty	0.01	0.08	0.03	0.08	0.10
GNG					
Experimental	7.53	0.99	2.88	1.39	11.21
Gaussian	7.49	0.97	3.05	1.41	11.24
Amber ff19SB	6.68	1.46	1.83	1.37	10.71
Amber ff14SB	6.50	1.00	1.83	1.78	11.05
OPLS-AA/M	7.41	0.76	2.36	1.56	10.98
CHARMM36m	6.92	0.91	2.38	1.67	10.99
Uncertainty	0.01	0.09	0.10	0.07	0.09
GSG					
Experimental	6.99	0.87	2.77	1.71	11.73
Gaussian	7.08	0.83	2.66	1.67	11.66

Amber ff149B	5.99	1.57	2.32	1.62	11.15
Amber ff14SB	6.62	1.34	2.25	1.50	10.99
OPLS-AA/M	7.23	0.92	2.24	1.52	11.07
CHARMM36m	6.82	1.28	2.23	1.45	11.07
Uncertainty	0.07	0.18	0.32	0.12	0.10
GTG					
Experimental	7.73	0.84	2.74	1.4	11.63
Gaussian	7.68	0.74	2.88	1.47	11.47
Amber ff19SB	7.17	1.50	2.13	1.14	11.02
Amber ff14SB	6.73	1.25	1.91	1.49	11.14
OPLS-AA/M	7.22	0.61	1.98	1.74	10.95
CHARMM36m	6.71	1.27	1.98	1.49	11.21
Uncertainty	0.02	0.08	0.05	0.12	0.10

^a Data taken from Andrews *et al.* [1].

^b Data taken from Zhang *et al.* [2].

Table S2: Mesostate populations of all guest amino acid residues in GxG considered in this work.

Populations	pPII	βt	$a\beta$	α	pPII	βt	$a\beta$	α	pPII	βt	$a\beta$	α
Aliphatic Amino Acids												
		G^{GG} ^{a,b}				G^{AG} ^c				G^{LG}		
Gaussian model	0.46	0.13	0.01	0.06	0.59	0.16	0.02	0.02	0.43	0.18	0.01	0.00
Amber ff19SB	0.39	0.02	0.05	0.05	0.45	0.02	0.14	0.10	0.41	0.05	0.09	0.15
Amber ff14SB	0.36	0.05	0.09	0.05	0.55	0.07	0.13	0.09	0.49	0.09	0.05	0.12
OPLS-AA/M	0.27	0.15	0.13	0.02	0.48	0.15	0.11	0.03	0.52	0.19	0.05	0.02
CHARMM36m	0.48	0.02	0.01	0.04	0.55	0.09	0.12	0.06	0.51	0.13	0.05	0.07
		G^{VG}				G^{IG}						
Gaussian model	0.30	0.40	0.02	0.02	0.28	0.10	0.01	0.06				
Amber ff19SB	0.36	0.04	0.17	0.07	0.58	0.04	0.07	0.00				
Amber ff14SB	0.48	0.09	0.12	0.12	0.63	0.09	0.07	0.08				
OPLS-AA/M	0.54	0.19	0.04	0.03	0.50	0.20	0.08	0.04				
CHARMM36m	0.55	0.11	0.05	0.06	0.49	0.12	0.06	0.09				
Aromatic Ring Amino Acids												
		G^{FG}				G^{YG}						
Gaussian model	0.35	0.34	0.08	0.05	0.36	0.29	0.02	0.02				
Amber ff19SB	0.42	0.05	0.26	0.05	0.36	0.04	0.19	0.17				
Amber ff14SB	0.49	0.09	0.12	0.11	0.53	0.08	0.15	0.06				
OPLS-AA/M	0.45	0.19	0.10	0.02	0.44	0.19	0.12	0.01				
CHARMM36m	0.48	0.12	0.10	0.06	0.46	0.11	0.11	0.08				
Charged Amino Acids												
		G^{D^PG}				G^{E^PG}				G^{RG}		
Gaussian model	0.08	0.16	0.08	0.01	0.39	0.25	0.05	0.02	0.42	0.21	0.02	0.07
Amber ff19SB	0.11	0.04	0.07	0.03	0.43	0.04	0.18	0.09	0.41	0.03	0.11	0.18
Amber ff14SB	0.39	0.07	0.10	0.07	0.42	0.08	0.14	0.10	0.43	0.08	0.12	0.19
OPLS-AA/M	0.47	0.17	0.07	0.02	0.48	0.18	0.10	0.02	0.45	0.18	0.11	0.02
CHARMM36m	0.36	0.17	0.12	0.03	0.36	0.08	0.17	0.10	0.46	0.13	0.11	0.05
Polar Amino Acids												
		G^{CG}				G^{NG}				G^{SG}		
Gaussian model	0.20	0.17	0.02	0.01	0.33	0.23	0.05	0.01	0.33	0.30	0.01	0.01
Amber ff19SB	0.25	0.05	0.55	0.01	0.32	0.04	0.13	0.09	0.48	0.04	0.16	0.02
Amber ff14SB	0.49	0.06	0.09	0.11	0.51	0.08	0.09	0.10	0.36	0.06	0.19	0.10
OPLS-AA/M	0.48	0.15	0.09	0.02	0.44	0.17	0.09	0.02	0.43	0.14	0.13	0.03
CHARMM36m	0.52	0.10	0.08	0.05	0.45	0.13	0.06	0.05	0.37	0.09	0.19	0.05
		G^{TG}										
Gaussian model	0.16	0.32	0.03	0.01								
Amber ff19SB	0.31	0.06	0.26	0.02								
Amber ff14SB	0.41	0.08	0.23	0.09								
OPLS-AA/M	0.56	0.16	0.04	0.02								
CHARMM36m	0.46	0.11	0.21	0.03								

^a Data, aside from Amber ff19SB, taken from Andrews *et al.* [1].^b Includes both left and right-handed mesostate populations.^c Data, aside from Amber ff19SB, taken from Zhang *et al.* [2].

Table S3: Shannon entropy differences ΔS_I and ΔS_{II} . The first section shows the Shannon entropy difference between each of the four MD force fields and Gaussian model (ΔS_I) for the guest residue in GxG. The section shows the Shannon entropy difference between the guest residue in GxG and alanine in GAG (ΔS_{II}) for the Gaussian model and the three MD force fields. The data for GGG and GAG is taken from our previous work [1].

$\Delta S_I [J \text{ mol}^{-1} K^{-1}]$	Gaussian	Amber ff19SB	Amber ff14SB	OPLS-AA/M	CHARMM36m
ΔS_{GGG}^a	—	-1.02	4.90	5.07	-1.66
ΔS_{GAG}^a	—	-0.61	0.66	1.49	-0.83
ΔS_{GLG}	—	-2.04	0.08	-2.08	-1.58
ΔS_{GVG}	—	2.57	2.91	-0.17	0.91
ΔS_{GIG}	—	-5.70	-2.99	-0.25	-2.83
ΔS_{GFG}	—	-2.39	0.83	0.42	0.50
ΔS_{GYG}	—	-0.48	0.42	-0.58	0.50
ΔS_{GDPG}	—	0.97	2.58	0.33	0.75
ΔS_{GEPG}	—	-3.32	1.44	-0.74	-1.10
ΔS_{GRG}	—	-2.49	-0.91	-1.33	-1.75
ΔS_{GCG}	—	-6.95	-0.17	0.08	-1.75
ΔS_{GNG}	—	4.51	4.74	5.65	5.15
ΔS_{GSG}	—	0.81	5.07	5.24	4.40
ΔS_{GTG}	—	2.18	3.49	1.00	1.50
$\Delta S_{II} [J \text{ mol}^{-1} K^{-1}]$	Gaussian	Amber ff19SB	Amber ff14SB	OPLS-AA/M	CHARMM36m
$S_{GGG} - S_{GAG}^a$	3.24	2.86	7.48	6.81	2.41
$S_{GLG} - S_{GAG}$	1.25	-0.14	0.75	-2.33	0.50
$S_{GVG} - S_{GAG}$	-3.49	-0.27	-1.16	-5.15	-1.75
$S_{GIG} - S_{GAG}$	-1.00	-6.12	-4.57	-2.74	-2.99
$S_{GFG} - S_{GAG}$	-0.25	-2.05	-1.41	-1.33	1.08
$S_{GYG} - S_{GAG}$	-0.91	-0.76	-1.08	-2.99	0.42
$S_{GDPG} - S_{GAG}$	0.58	2.17	2.58	-0.58	2.16
$S_{GEPG} - S_{GAG}$	0.70	-2.01	1.50	-1.54	0.41
$S_{GRG} - S_{GAG}$	1.50	-0.41	0.00	-1.33	0.58
$S_{GCG} - S_{GAG}$	1.41	-4.94	0.67	0.00	0.50
$S_{GNG} - S_{GAG}$	-3.91	1.23	0.25	0.25	2.07
$S_{GSG} - S_{GAG}$	-2.24	-0.84	2.24	1.50	2.99
$S_{GTG} - S_{GAG}$	-2.74	0.07	0.17	-3.24	-0.42

^a Data taken from Andrews *et al.* [1].

Supporting Figures

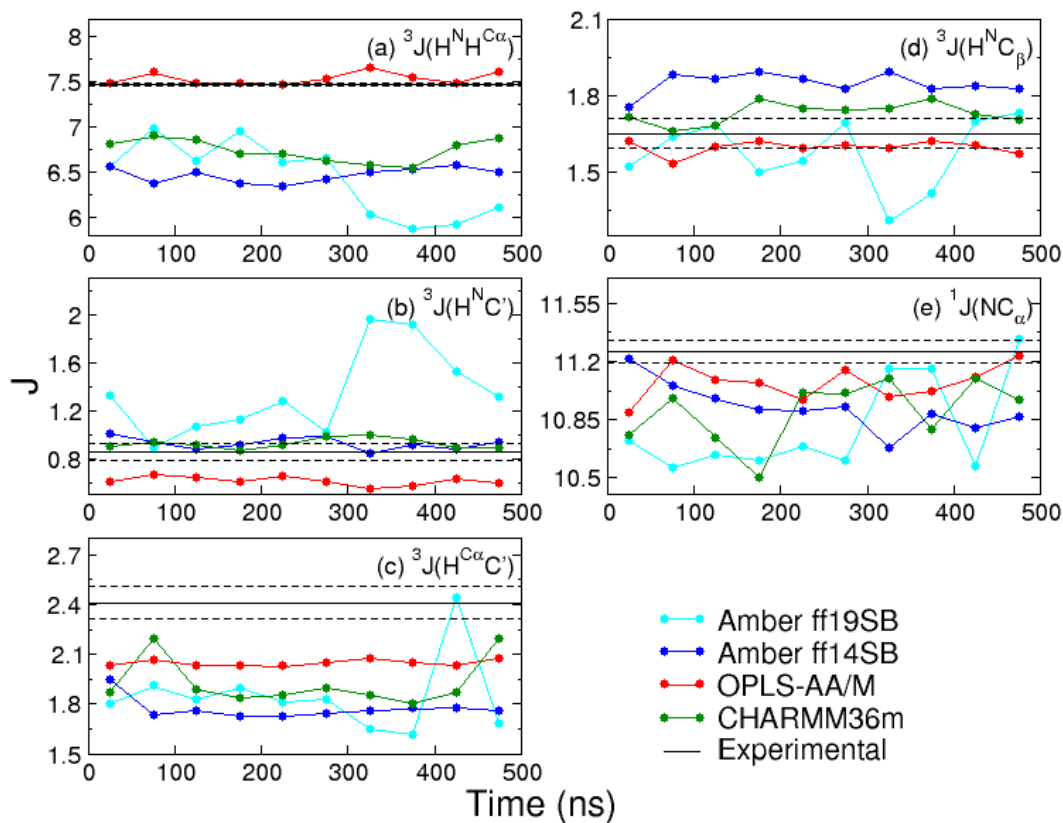


Figure S1: The five J-coupling constants of central isoleucine in GIG calculated in 50 ns intervals of the 300 ns trajectories in each force field to monitor simulation convergence. Black solid lines represent the experimental J-coupling constants (Table S1) and black dashed lines represent the uncertainties (Table S1).

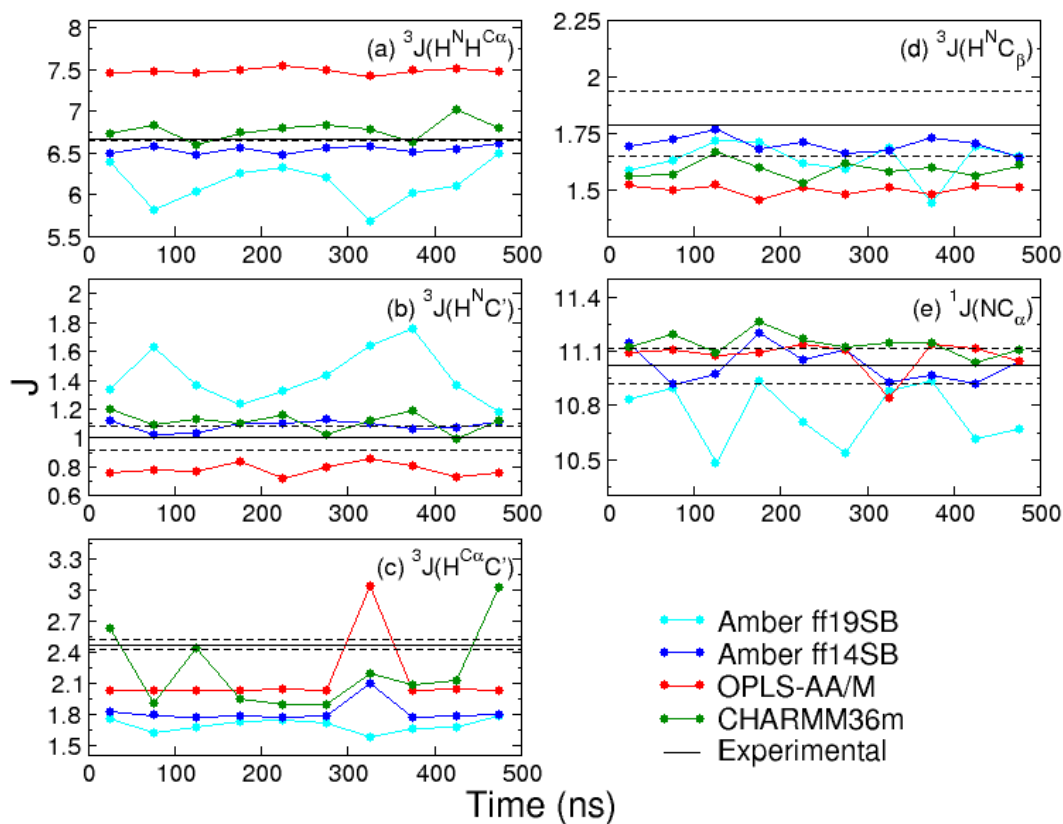


Figure S2: The five J-coupling constants of central arginine in GRG calculated in 50 ns intervals of the 300 ns trajectories in each force field to monitor simulation convergence. Black solid lines represent the experimental J-coupling constants (Table S1) and black dashed lines represent the uncertainties (Table S1).

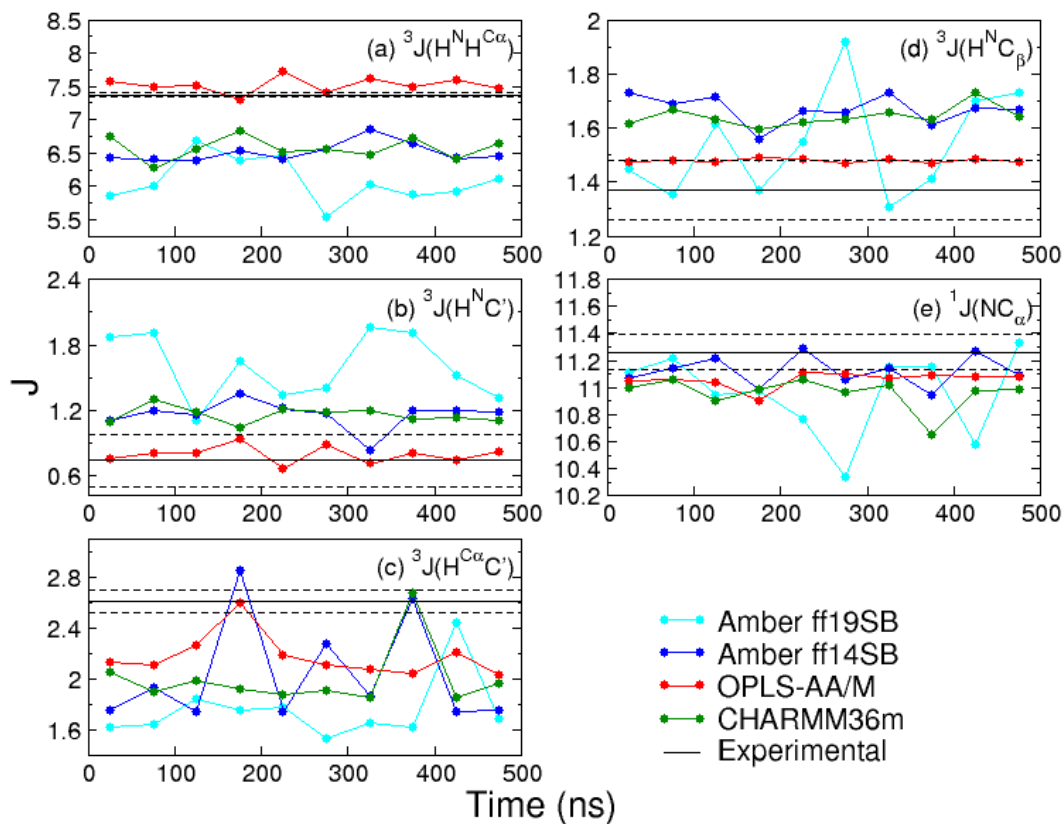


Figure S3: The five J-coupling constants of central tyrosine in GYG calculated in 50 ns intervals of the 300 ns trajectories in each force field to monitor simulation convergence. Black solid lines represent the experimental J-coupling constants (Table S1) and black dashed lines represent the uncertainties (Table S1).

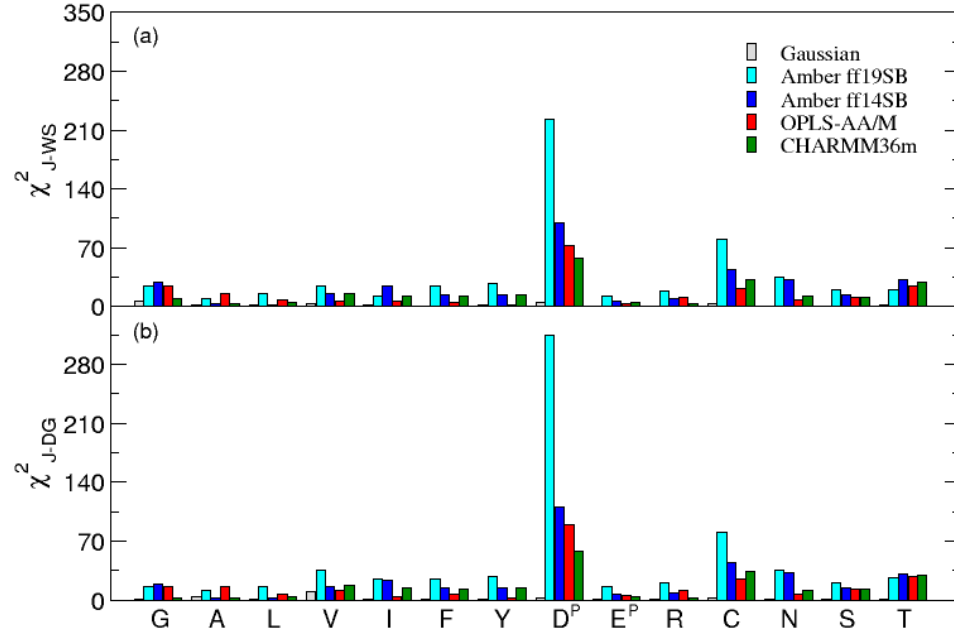


Figure S4: Assessment of the Gaussian model and four MD force fields with respect to their ability to reproduce the experimental data for the guest residue in cationic GxG using χ^2_J with the (a) Wirmer-Schwalbe [3] and (b) Ding-Gronenborn [4] parameters for $^1J(N, C_\alpha)$. Values presented for GGG and GAG in (a), aside from those for Amber ff19SB, are taken from our previous works [1, 2].

Aliphatic Amino Acids

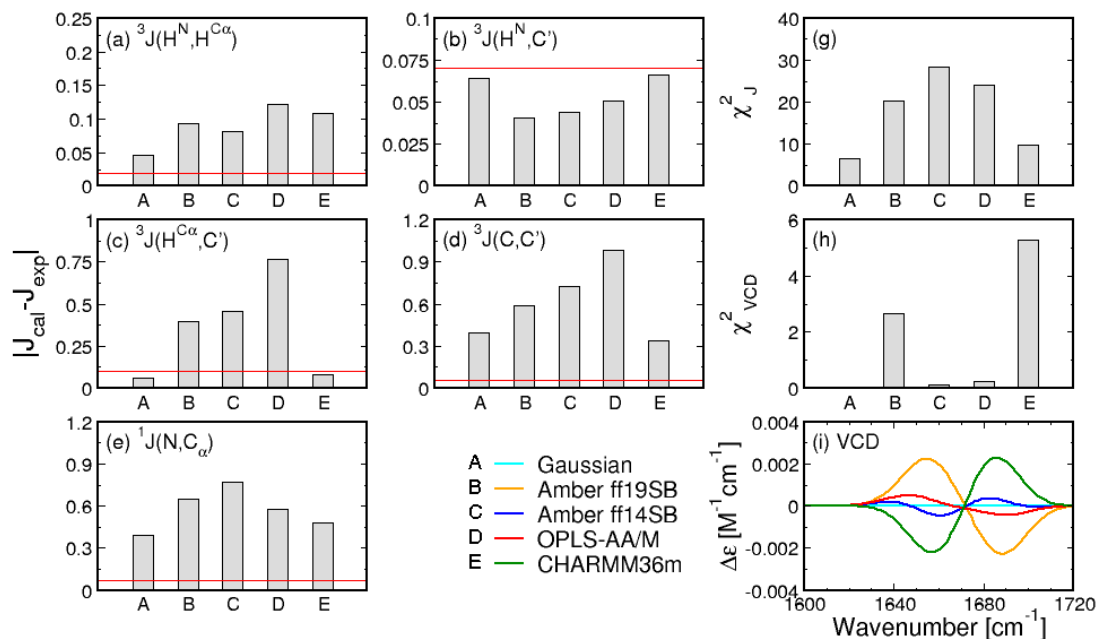


Figure S5: A comparison between experimental and calculated J-coupling constants and amide I' profiles of the Gaussian model and four MD force fields for glycine in GGG. (a-e) Absolute differences between calculated and experimental values of the five J-coupling constants for the Gaussian model and the three MD force fields. Red lines correspond to experimental uncertainties. (f) A comparison between experimental and calculated amide I' profiles. (g,h) The two χ^2 functions. Data for GGG with Amber ff19SB is compared to data from our previous work [1].

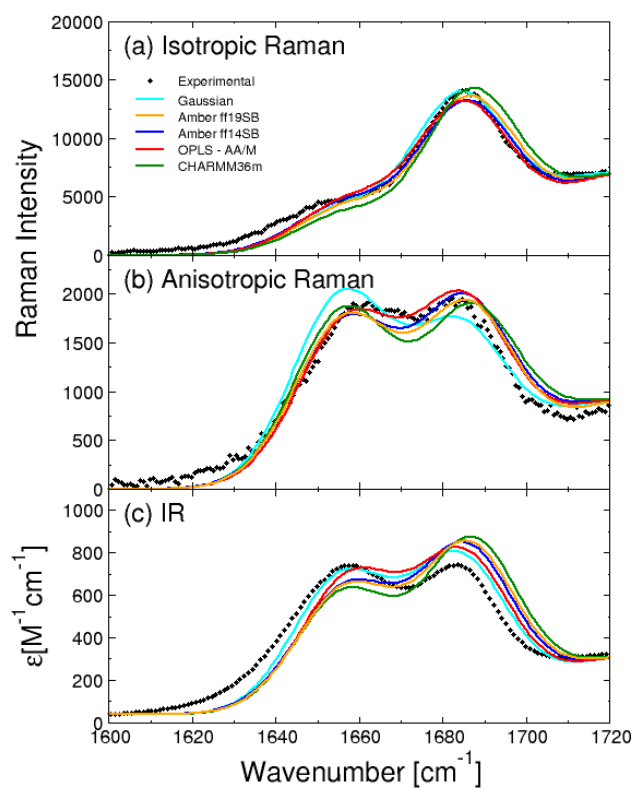


Figure S6: Amide I' profiles for the leucine in GGG. Experimental amide I' profiles derived from (a) isotropic Raman, (b) anisotropic Raman, and (c) IR spectroscopy measurements are compared to predictions of the Gaussian model and MD simulations with Amber ff19SB, Amber ff14SB, OPLS-AA/M, and CHARMM36m. Data for GGG with Amber ff19SB is compared to data from our previous work [1].

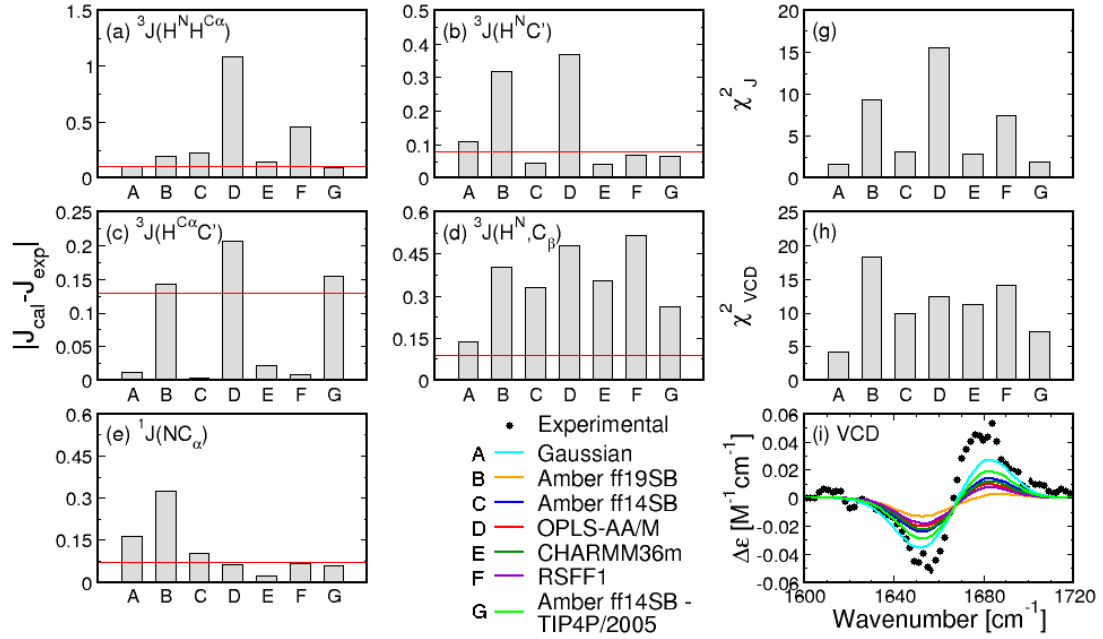


Figure S7: A comparison between experimental and calculated J-coupling constants and amide I' profiles of the Gaussian model and four MD force fields for alanine in GAG. (a-e) Absolute differences between calculated and experimental values of the five J-coupling constants for the Gaussian model and the three MD force fields. Red lines correspond to experimental uncertainties. (f) A comparison between experimental and calculated amide I' profiles. (g,h) The two χ^2 functions. Data for GAG with Amber ff19SB is compared to data from our previous work [2].

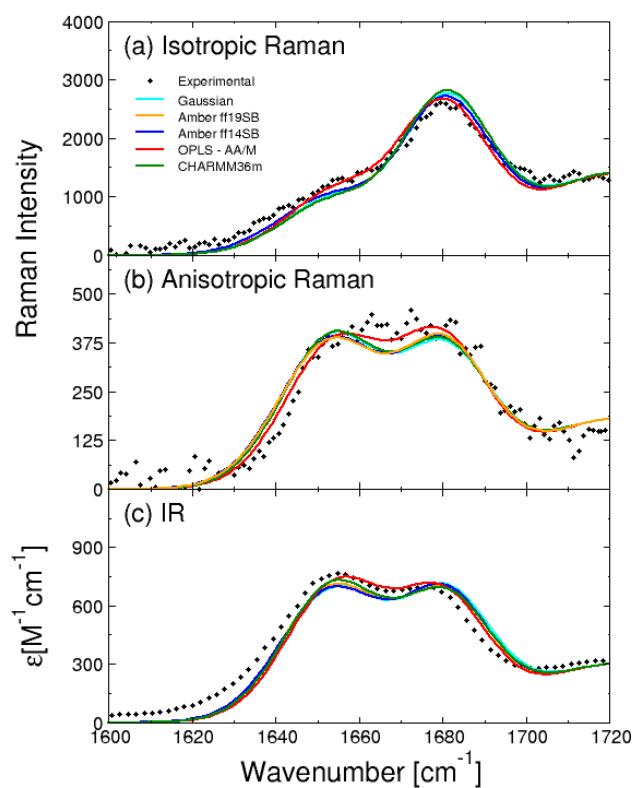


Figure S8: Amide I' profiles for the leucine in GAG. Experimental amide I' profiles derived from (a) isotropic Raman, (b) anisotropic Raman, and (c) IR spectroscopy measurements are compared to predictions of the Gaussian model and MD simulations with Amber ff19SB, Amber ff14SB, OPLS-AA/M, and CHARMM36m. Data for GAG with Amber ff19SB is compared to data from our previous work [2].

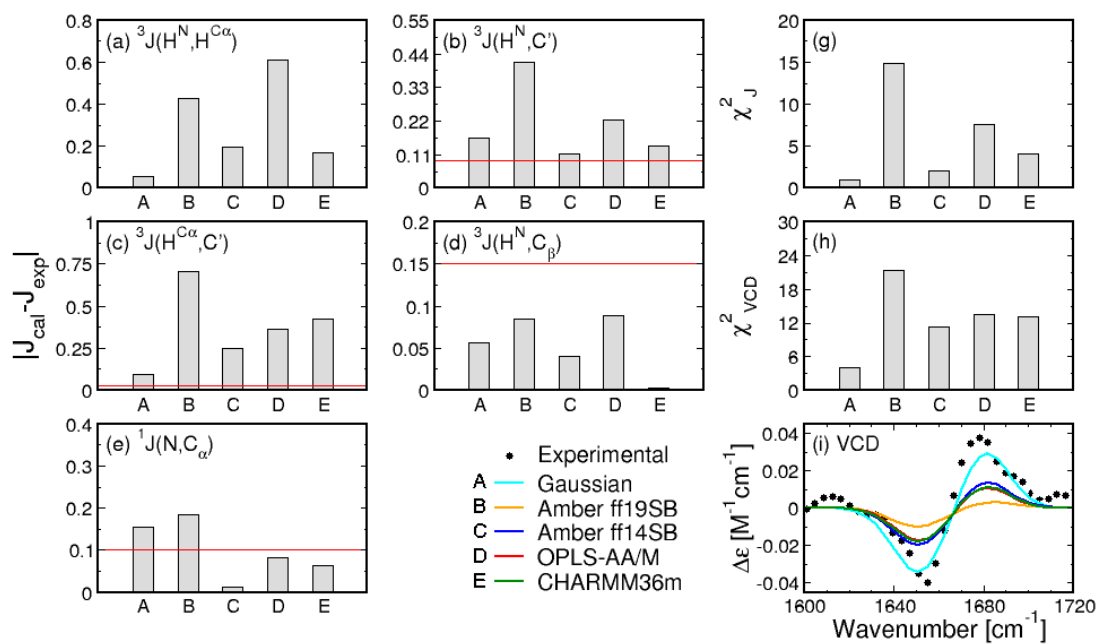


Figure S9: A comparison between experimental and calculated J-coupling constants and amide I' profiles of the Gaussian model and four MD force fields for leucine in GLG. (a-e) Absolute differences between calculated and experimental values of the five J-coupling constants for the Gaussian model and the three MD force fields. Red lines correspond to experimental uncertainties. (f) A comparison between experimental and calculated amide I' profiles. (g,h) The two χ^2 functions.

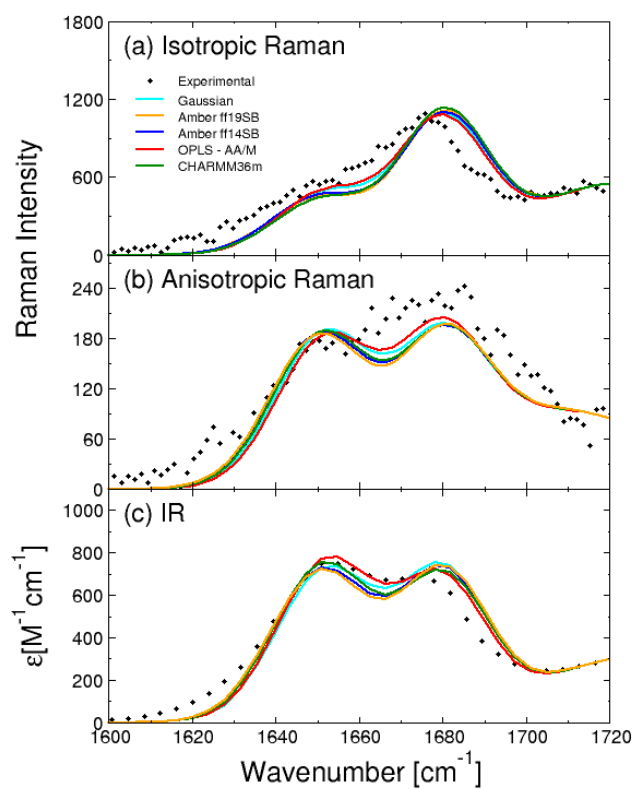


Figure S10: Amide I' profiles for the leucine in GLG. Experimental amide I' profiles derived from (a) isotropic Raman, (b) anisotropic Raman, and (c) IR spectroscopy measurements are compared to predictions of the Gaussian model and MD simulations with Amber ff19SB, Amber ff14SB, OPLS-AA/M, and CHARMM36m.

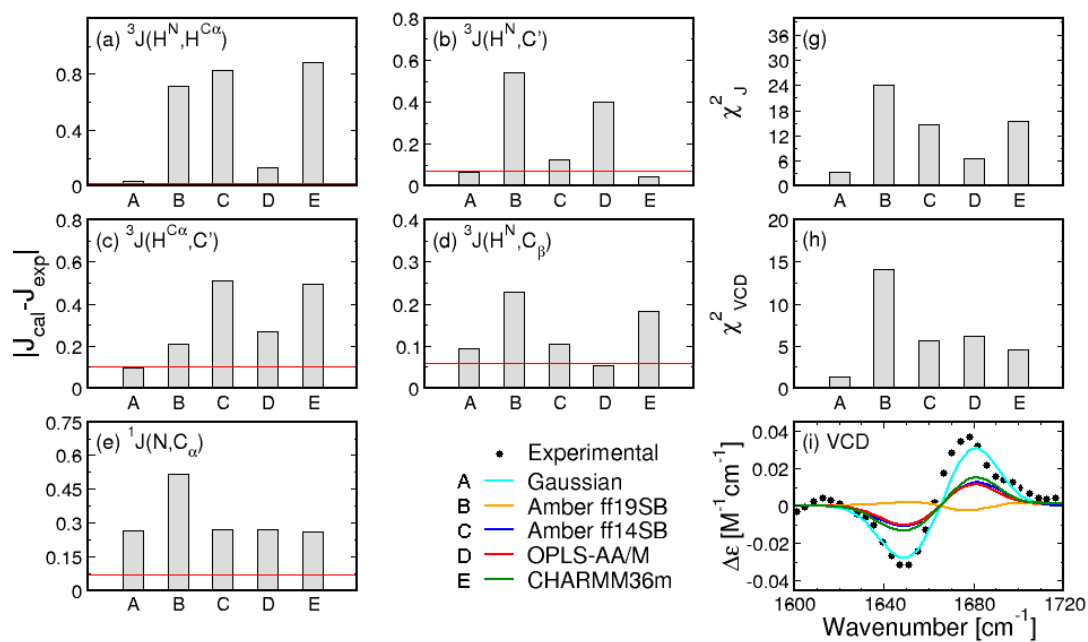


Figure S11: A comparison between experimental and calculated J-coupling constants and amide I' profiles of the Gaussian model and four MD force fields for valine in GVG. (a-e) Absolute differences between calculated and experimental values of the five J-coupling constants for the Gaussian model and the three MD force fields. Red lines correspond to experimental uncertainties. (f) A comparison between experimental and calculated amide I' profiles. (g,h) The two χ^2 functions.

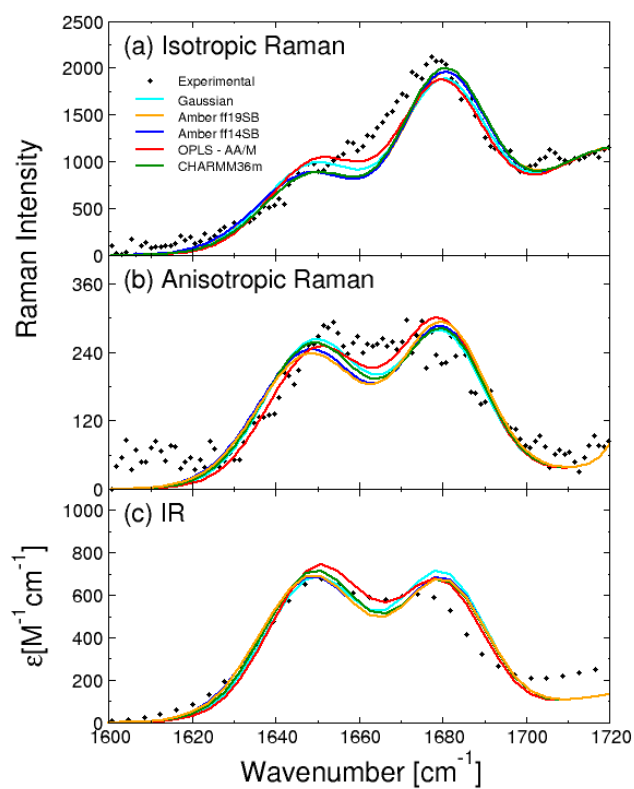


Figure S12: Amide I' profiles for the valine in GVG. Experimental amide I' profiles derived from (a) isotropic Raman, (b) anisotropic Raman, and (c) IR spectroscopy measurements are compared to predictions of the Gaussian model and MD simulations with Amber ff19SB, Amber ff14SB, OPLS-AA/M, and CHARMM36m.

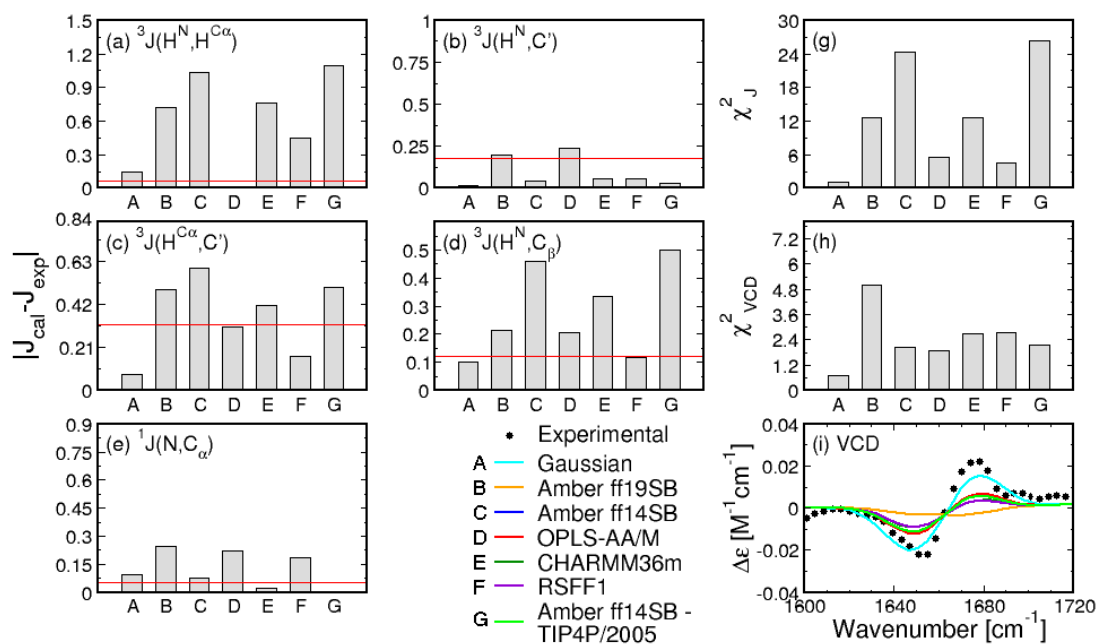


Figure S13: A comparison between experimental and calculated J-coupling constants and amide I' profiles of the Gaussian model and four MD force fields for isoleucine in GIG. (a-e) Absolute differences between calculated and experimental values of the five J-coupling constants for the Gaussian model and the three MD force fields. Red lines correspond to experimental uncertainties. (f) A comparison between experimental and calculated amide I' profiles. (g,h) The two χ^2 functions.

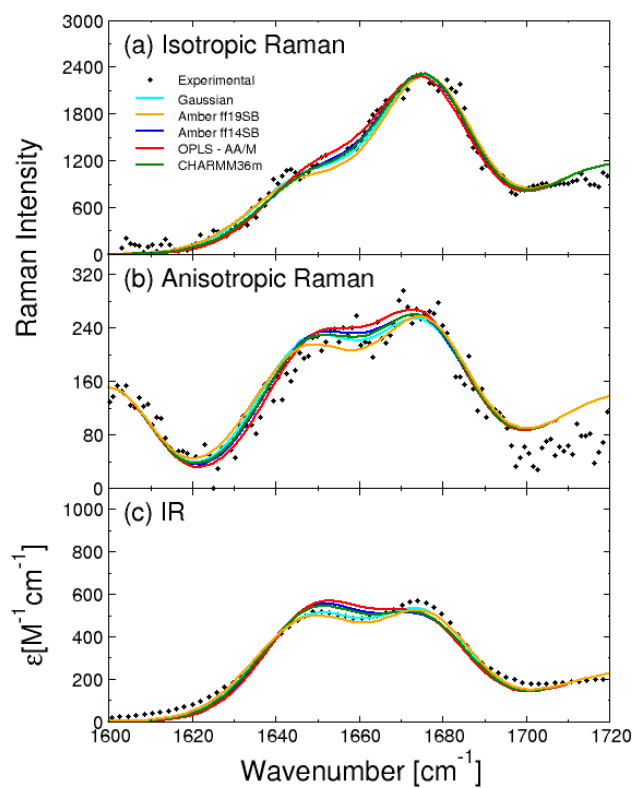


Figure S14: Amide I' profiles for the isoleucine in GIG. Experimental amide I' profiles derived from (a) isotropic Raman, (b) anisotropic Raman, and (c) IR spectroscopy measurements are compared to predictions of the Gaussian model and MD simulations with Amber ff19SB, Amber ff14SB, OPLS-AA/M, and CHARMM36m.

Aromatic Amino Acids

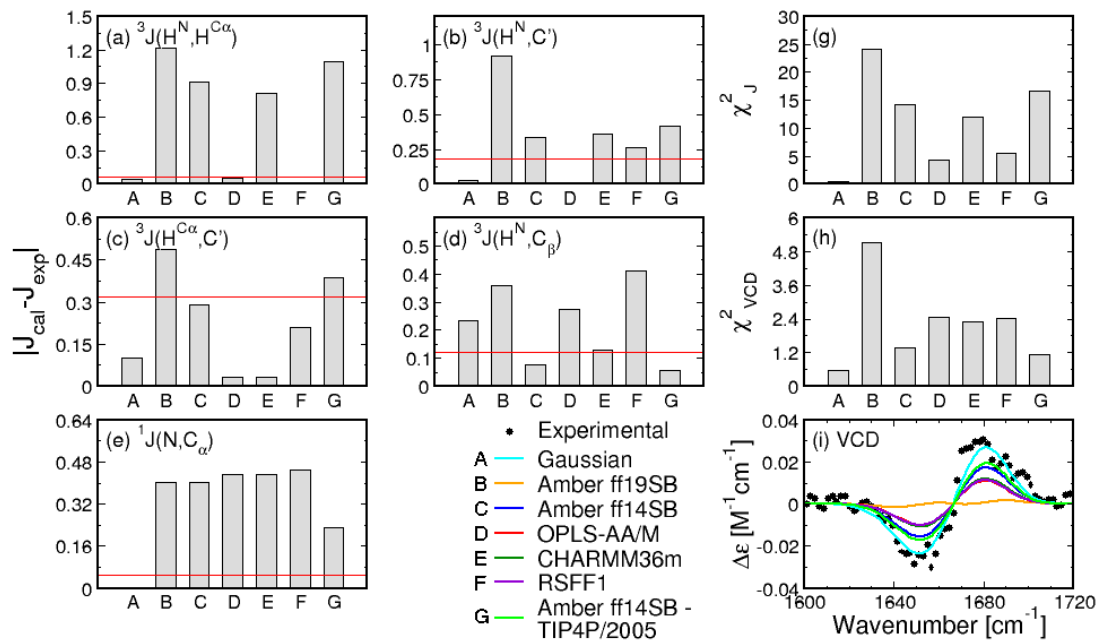


Figure S15: A comparison between experimental and calculated J-coupling constants and amide I' profiles of the Gaussian model and four MD force fields for phenylalanine in GFG. (a-e) Absolute differences between calculated and experimental values of the five J-coupling constants for the Gaussian model and the three MD force fields. Red lines correspond to experimental uncertainties. (f) A comparison between experimental and calculated amide I' profiles. (g,h) The two χ^2 functions.

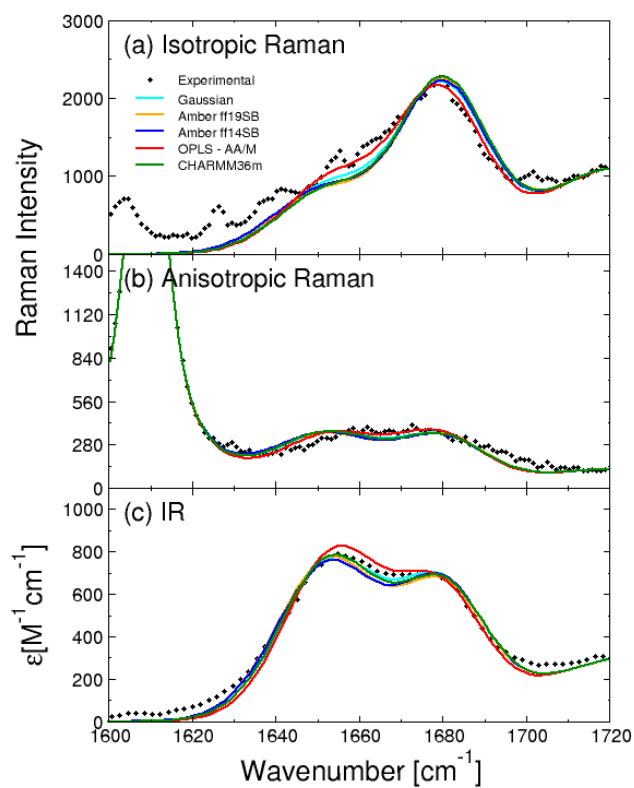


Figure S16: Amide I' profiles for the phenylalanine in GFG. Experimental amide I' profiles derived from (a) isotropic Raman, (b) anisotropic Raman, and (c) IR spectroscopy measurements are compared to predictions of the Gaussian model and MD simulations with Amber ff19SB, Amber ff14SB, OPLS-AA/M, and CHARMM36m.

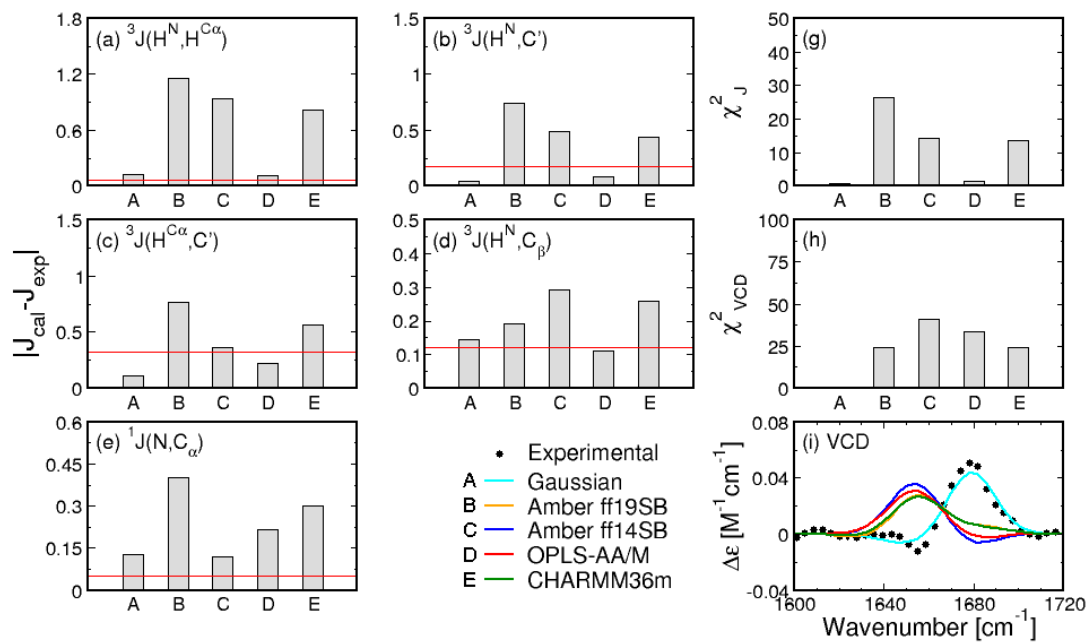


Figure S17: A comparison between experimental and calculated J-coupling constants and amide I' profiles of the Gaussian model and four MD force fields for tyrosine in GYG. (a-e) Absolute differences between calculated and experimental values of the five J-coupling constants for the Gaussian model and the three MD force fields. Red lines correspond to experimental uncertainties. (f) A comparison between experimental and calculated amide I' profiles. (g,h) The two χ^2 functions.

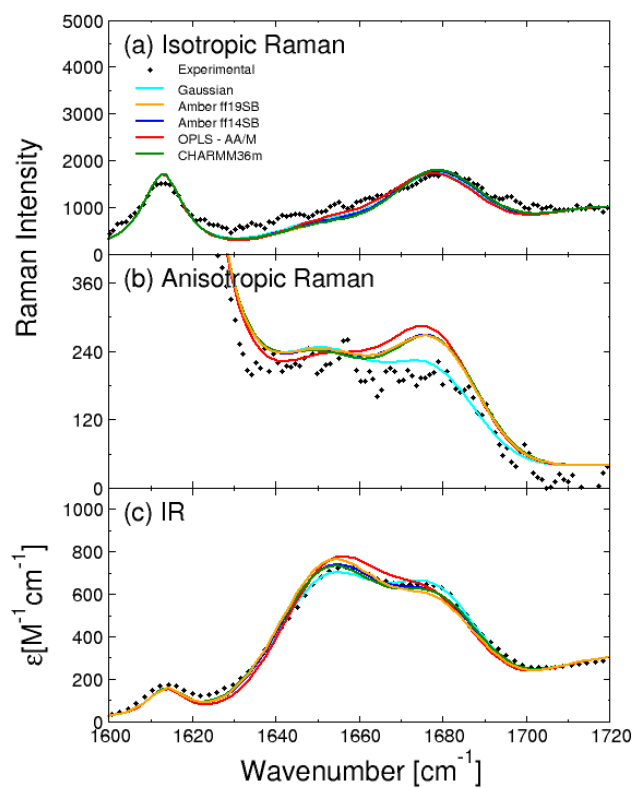


Figure S18: Amide I' profiles for the tyrosine in GYG. Experimental amide I' profiles derived from (a) isotropic Raman, (b) anisotropic Raman, and (c) IR spectroscopy measurements are compared to predictions of the Gaussian model and MD simulations with Amber ff19SB, Amber ff14SB, OPLS-AA/M, and CHARMM36m.

Ionizable Amino Acids

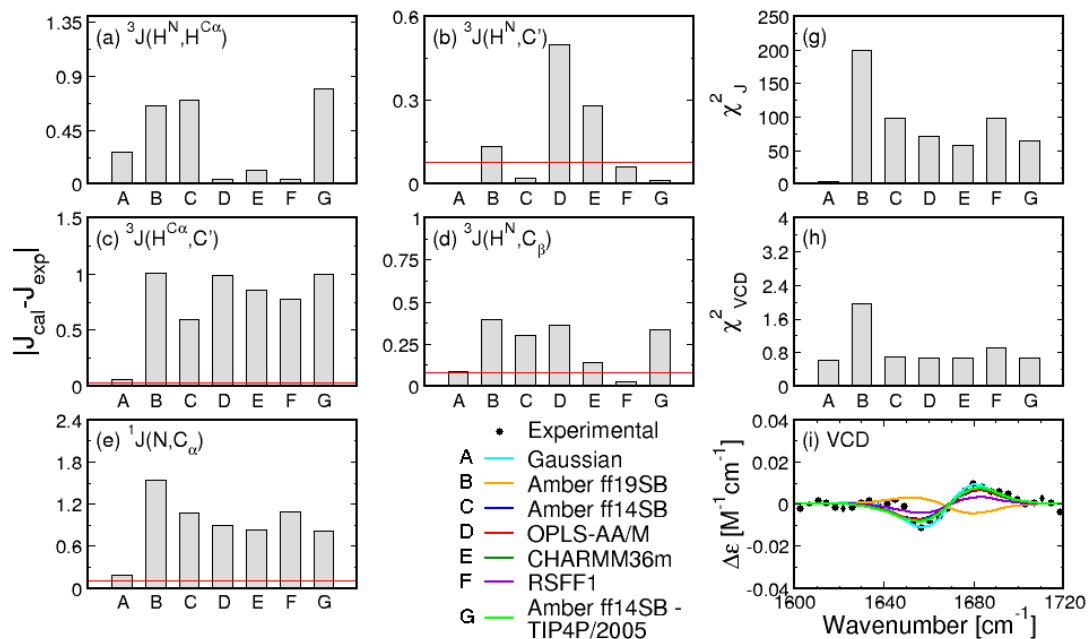


Figure S19: A comparison between experimental and calculated J-coupling constants and amide I' profiles of the Gaussian model and four MD force fields for protonated aspartic acid in GD^PG (a-e). Absolute differences between calculated and experimental values of the five J-coupling constants for the Gaussian model and the three MD force fields. Red lines correspond to experimental uncertainties. (f) A comparison between experimental and calculated amide I' profiles. (g,h) The two χ^2 functions.

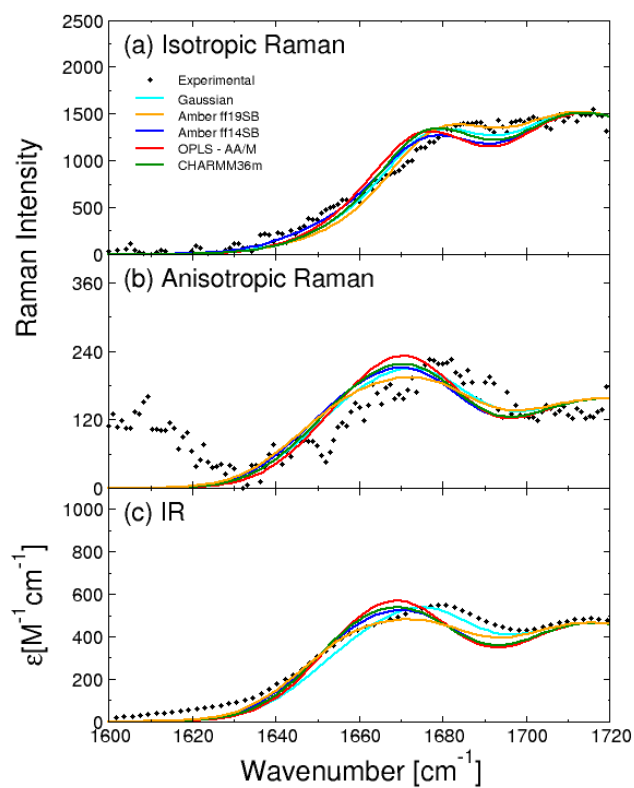


Figure S20: Amide I' profiles for protonated aspartic acid in $GD^P G$. Experimental amide I' profiles derived from (a) isotropic Raman, (b) anisotropic Raman, and (c) IR spectroscopy measurements are compared to predictions of the Gaussian model and MD simulations with Amber ff19SB, Amber ff14SB, OPLS-AA/M, and CHARMM36m.

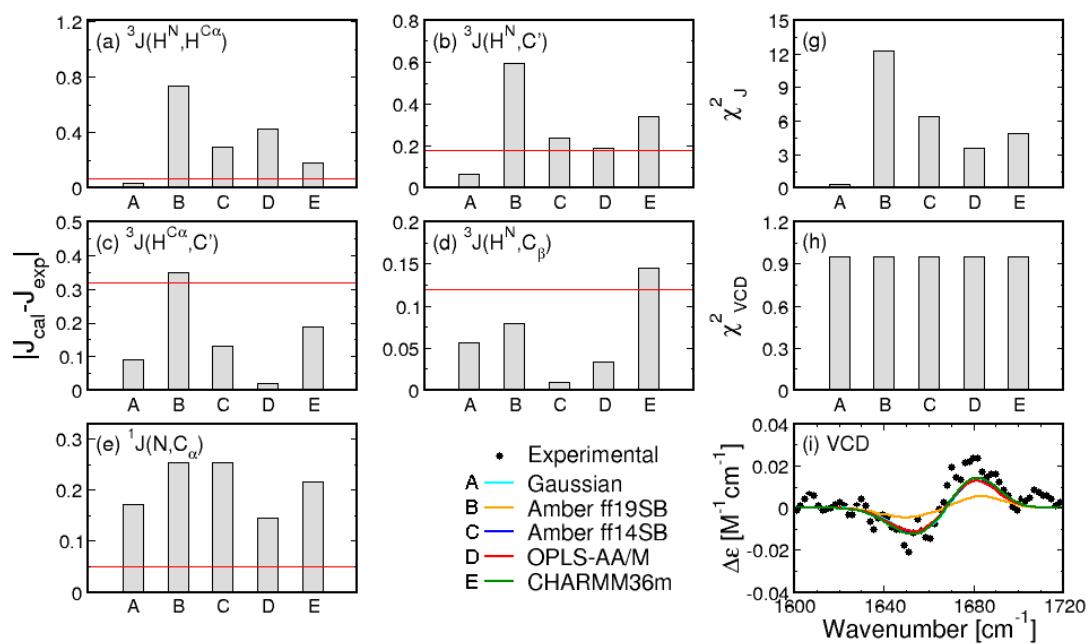


Figure S21: A comparison between experimental and calculated J-coupling constants and amide I' profiles of the Gaussian model and four MD force fields for protonated glutamic acid in GE^PG . (a-e) Absolute differences between calculated and experimental values of the five J-coupling constants for the Gaussian model and the three MD force fields. Red lines correspond to experimental uncertainties. (f) A comparison between experimental and calculated amide I' profiles. (g,h) The two χ^2 functions.

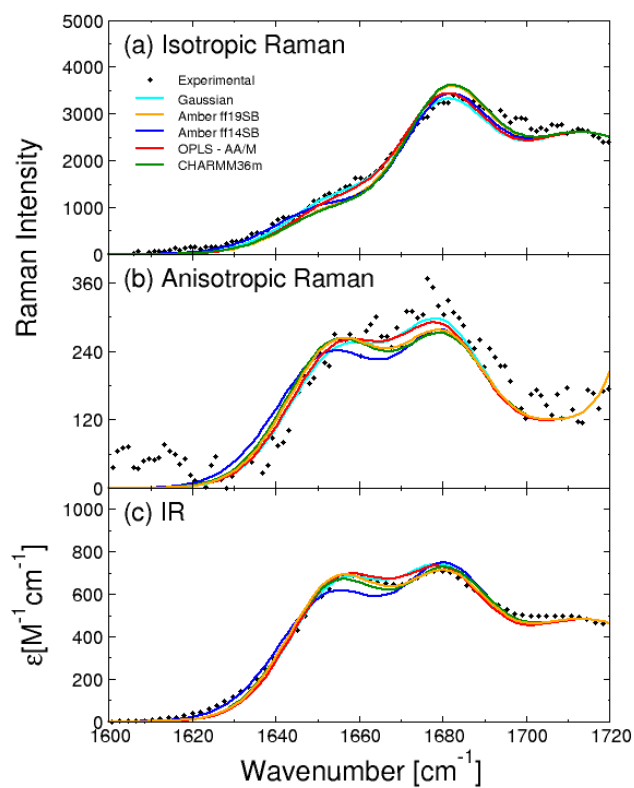


Figure S22: Amide I' profiles for protonated glutamic acid in $GE^P G$. Experimental amide I' profiles derived from (a) isotropic Raman, (b) anisotropic Raman, and (c) IR spectroscopy measurements are compared to predictions of the Gaussian model and MD simulations with Amber ff19SB, Amber ff14SB, OPLS-AA/M, and CHARMM36m.

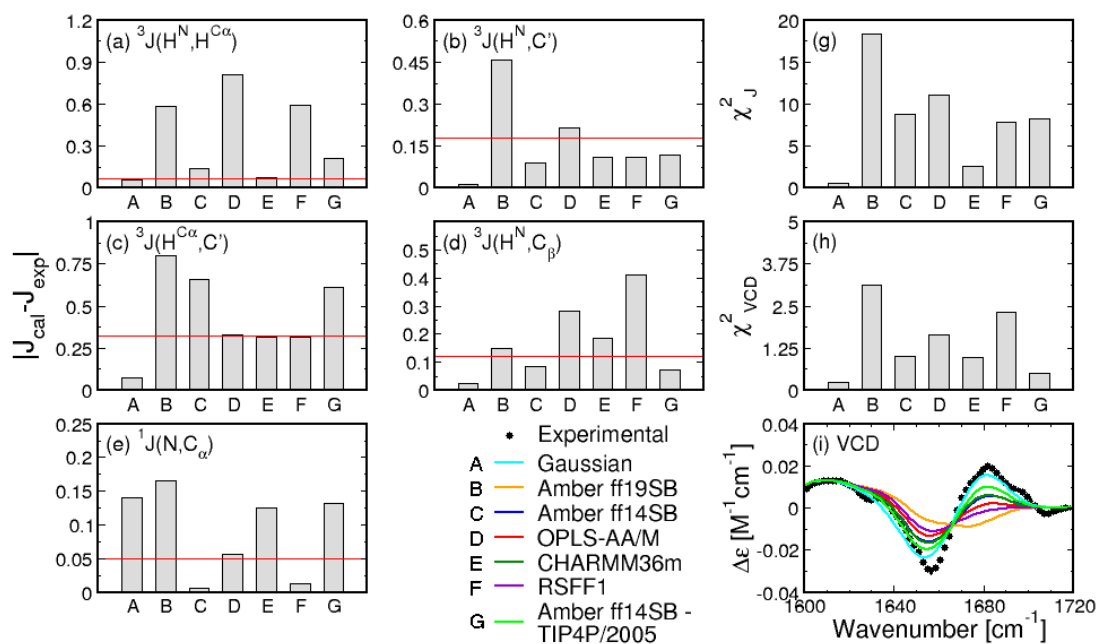


Figure S23: A comparison between experimental and calculated J-coupling constants and amide I' profiles of the Gaussian model and four MD force fields for arginine in GRG. (a-e) Absolute differences between calculated and experimental values of the five J-coupling constants for the Gaussian model and the three MD force fields. Red lines correspond to experimental uncertainties. (f) A comparison between experimental and calculated amide I' profiles. (g,h) The two χ^2 functions.

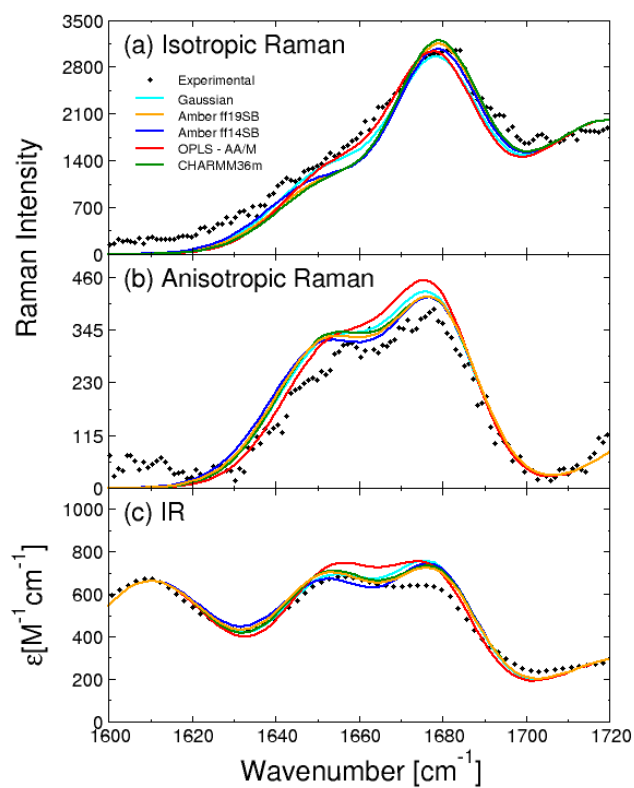


Figure S24: Amide I' profiles for the arginine in GRG. Experimental amide I' profiles derived from (a) isotropic Raman, (b) anisotropic Raman, and (c) IR spectroscopy measurements are compared to predictions of the Gaussian model and MD simulations with Amber ff19SB, Amber ff14SB, OPLS-AA/M, and CHARMM36m.

Polar Amino Acids

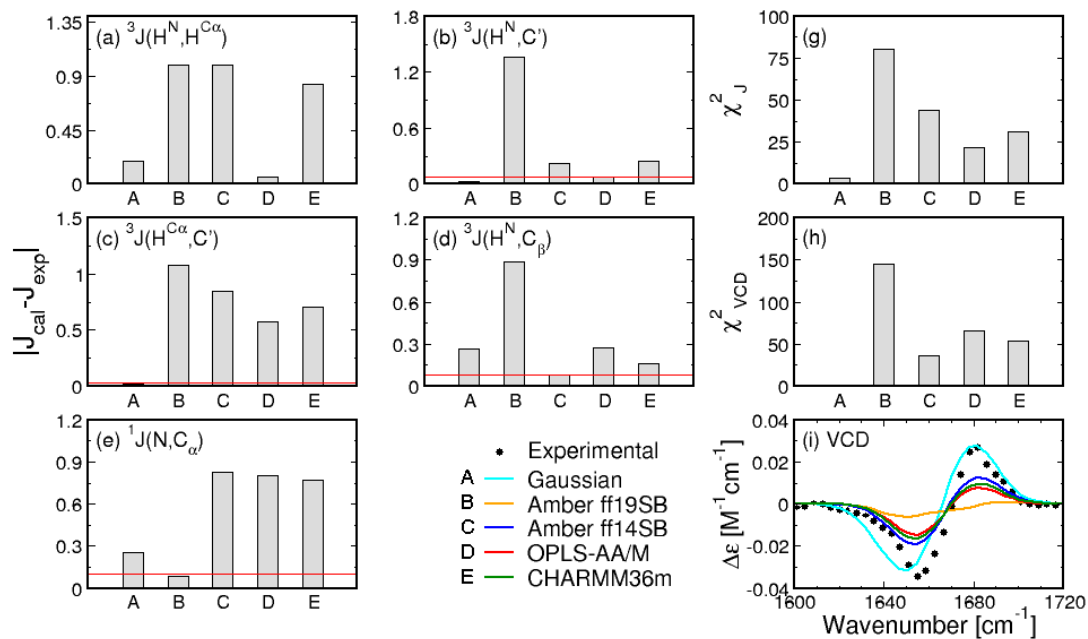


Figure S25: A comparison between experimental and calculated J-coupling constants and amide I' profiles of the Gaussian model and four MD force fields for cysteine in GCG. (a-e) Absolute differences between calculated and experimental values of the five J-coupling constants for the Gaussian model and the three MD force fields. Red lines correspond to experimental uncertainties. (f) A comparison between experimental and calculated amide I' profiles. (g,h) The two χ^2 functions.

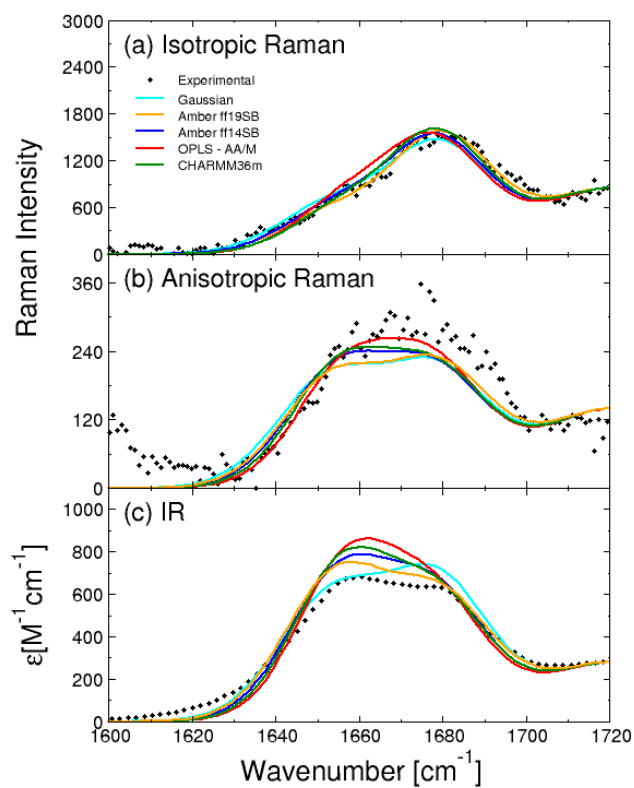


Figure S26: Amide I' profiles for the cysteine in GCG. Experimental amide I' profiles derived from (a) isotropic Raman, (b) anisotropic Raman, and (c) IR spectroscopy measurements are compared to predictions of the Gaussian model and MD simulations with Amber ff19SB, Amber ff14SB, OPLS-AA/M, and CHARMM36m.

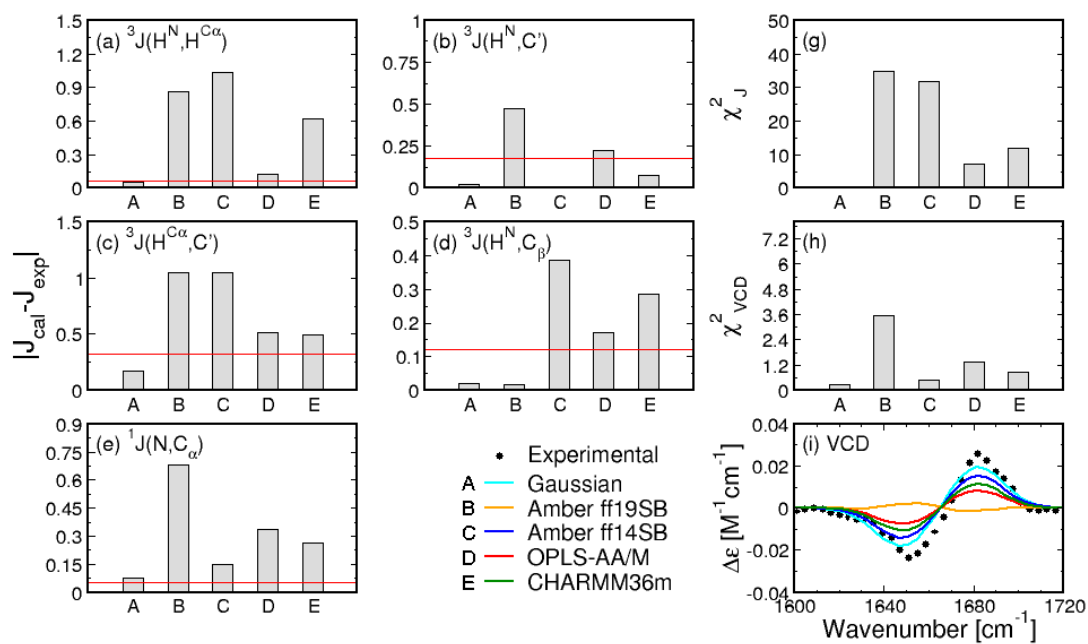


Figure S27: A comparison between experimental and calculated J-coupling constants and amide I' profiles of the Gaussian model and four MD force fields for asparagine in GNG. (a-e) Absolute differences between calculated and experimental values of the five J-coupling constants for the Gaussian model and the three MD force fields. Red lines correspond to experimental uncertainties. (f) A comparison between experimental and calculated amide I' profiles. (g,h) The two χ^2 functions.

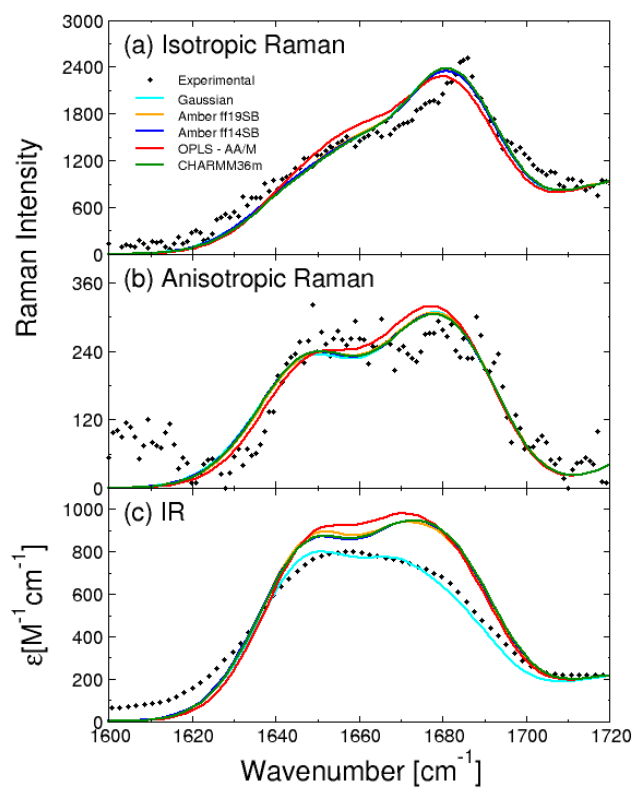


Figure S28: Amide I' profiles for the asparagine in GNG. Experimental amide I' profiles derived from (a) isotropic Raman, (b) anisotropic Raman, and (c) IR spectroscopy measurements are compared to predictions of the Gaussian model and MD simulations with Amber ff19SB, Amber ff14SB, OPLS-AA/M, and CHARMM36m.

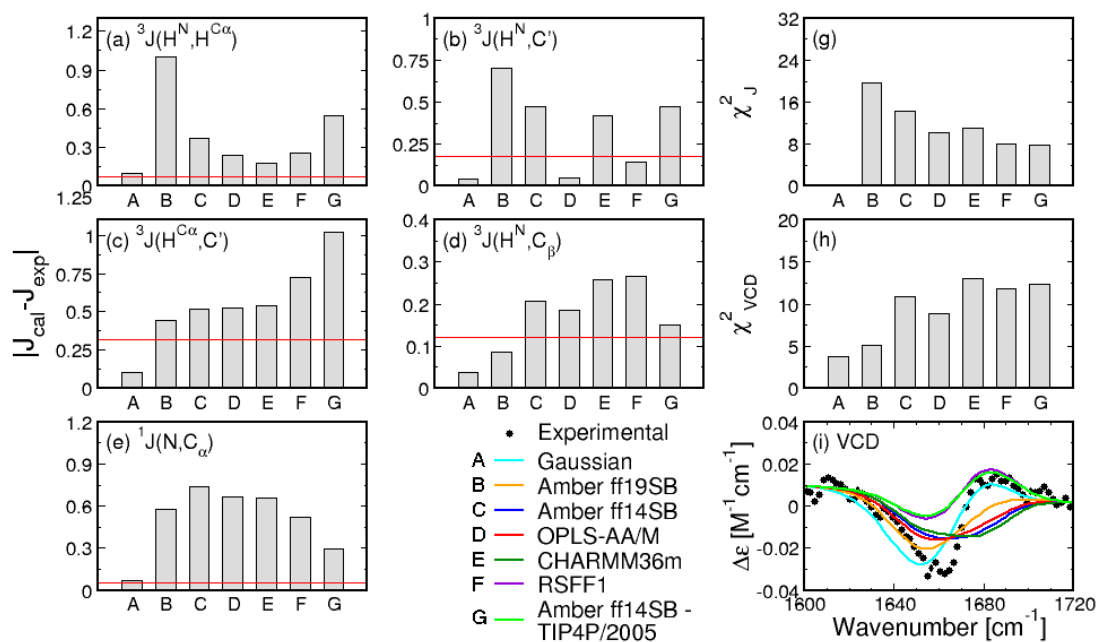


Figure S29: A comparison between experimental and calculated J-coupling constants and amide I' profiles of the Gaussian model and four MD force fields for serine in GSG. (a-e) Absolute differences between calculated and experimental values of the five J-coupling constants for the Gaussian model and the three MD force fields. Red lines correspond to experimental uncertainties. (f) A comparison between experimental and calculated amide I' profiles. (g,h) The two χ^2 functions.

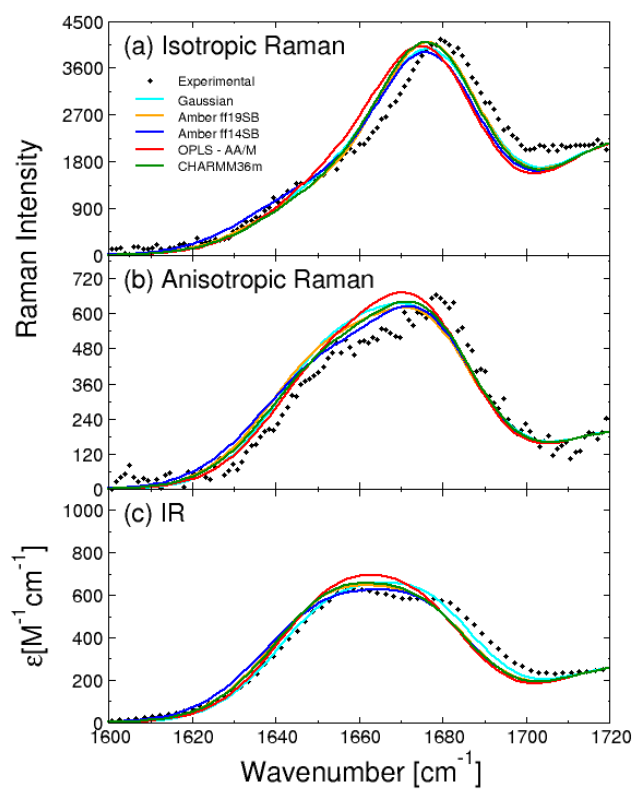


Figure S30: Amide I' profiles for the serine in GSG. Experimental amide I' profiles derived from (a) isotropic Raman, (b) anisotropic Raman, and (c) IR spectroscopy measurements are compared to predictions of the Gaussian model and MD simulations with Amber ff19SB, Amber ff14SB, OPLS-AA/M, and CHARMM36m.

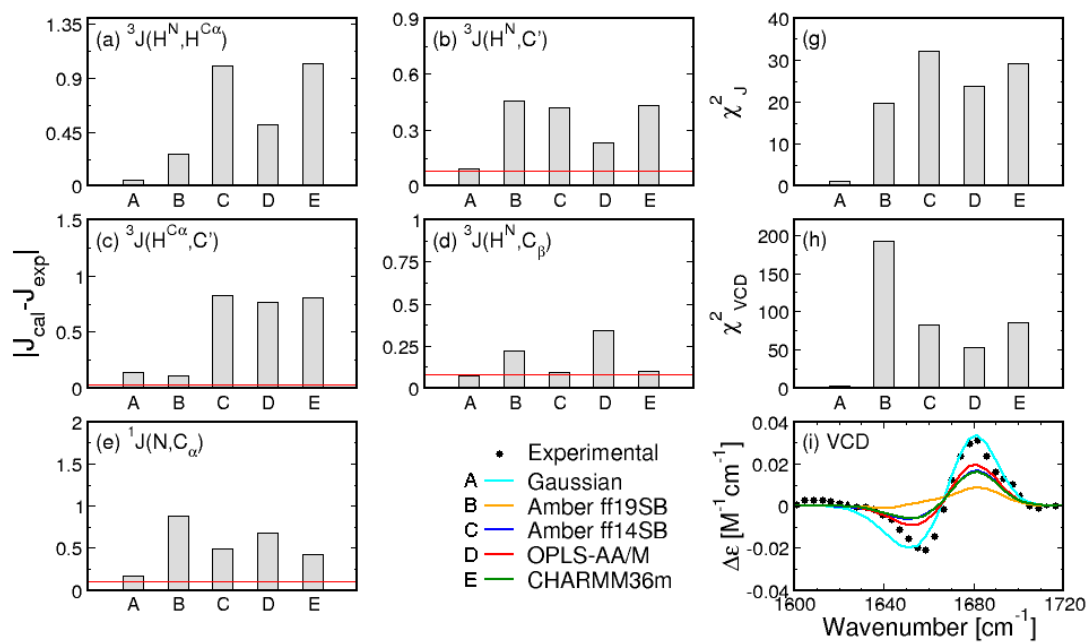


Figure S31: A comparison between experimental and calculated J-coupling constants and amide I' profiles of the Gaussian model and four MD force fields for threonine in GTG. (a-e) Absolute differences between calculated and experimental values of the five J-coupling constants for the Gaussian model and the three MD force fields. Red lines correspond to experimental uncertainties. (f) A comparison between experimental and calculated amide I' profiles. (g,h) The two χ^2 functions.

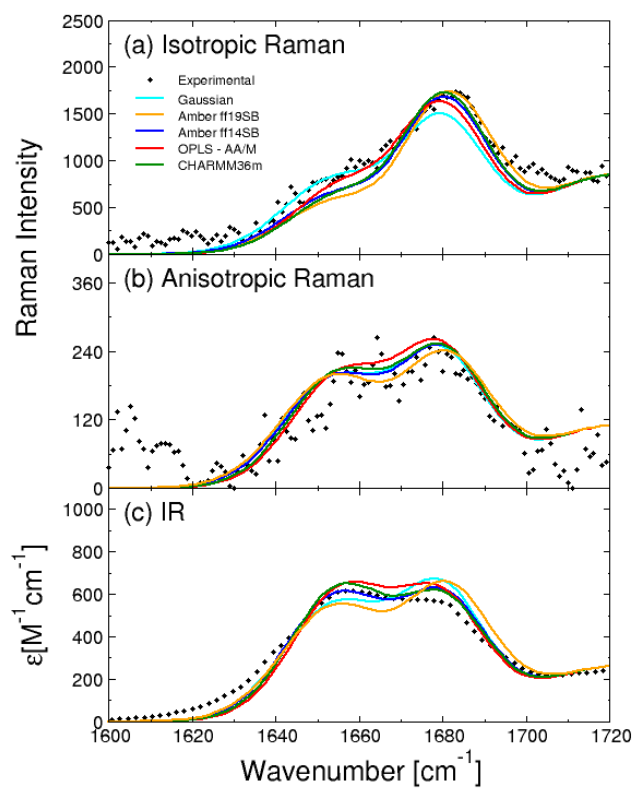


Figure S32: Amide I' profiles for the threonine in GTG. Experimental amide I' profiles derived from (a) isotropic Raman, (b) anisotropic Raman, and (c) IR spectroscopy measurements are compared to predictions of the Gaussian model and MD simulations with Amber ff19SB, Amber ff14SB, OPLS-AA/M, and CHARMM36m.

References

- [1] B. Andrews, S. Zhang, R. Schweitzer-Stenner, and B. Urbanc. Glycine in water favors the polyproline II state,. *Biomolecules*, 10:1121, 2020.
- [2] Shuting Zhang, Reinhard Schweitzer-Stenner, and Brigita Urbanc. Do molecular dynamics force fields capture conformational dynamics of alanine in water? *J. Chem. Theory Comput.*, 16:510–527, 2020.
- [3] J. Wirmer and H. Schwalbe. Angular dependence of $^1J(N_i, C_{\alpha i})$ and $^2J(N_i, C_{\alpha(i-1)})$ coupling constants measured in J-modulated HSQCs. *J. Biomol. NMR*, 23(1):47–55, MAY 2002.
- [4] J.-S. Hu and A. Bax. Determination of ϕ and χ_1 angles in proteins from ^{13}C – ^{13}C three-bond J couplings measured by three-dimensional heteronuclear NMR. How planar is the peptide bond? *J. Am. Chem. Soc.*, 119(27):6360–6368, JUL 9 1997.